Correlation for Mold Heat Flux Measured in a Thin Slab Casting Mold

Prathiba Duvvuri, Bryan Petrus, and Brian G. Thomas

Department of Mechanical Science and Engineering
University of Illinois at Urbana-Champaign
1206 W. Green Street
Urbana, IL 61801 USA
Phone - (217) 333-6919
Fax - (217) 244-6534
Email: bgthomas@uiuc.edu

Keywords: Continuous casting, Thin slab caster, Mold heat flux, Non-linear multiple regression

INTRODUCTION

Maintaining appropriate heat transfer in the steel continuous casting mold is critical to strand surface quality [1-3], mold life [4], casting productivity [5] and operating safety in preventing breakouts [6,7]. Considerable research on mold heat transfer has been based on computational modeling and numerical simulations. However, with advances in mold instrumentation and data collection, plant measurements can be analyzed to investigate these phenomena in actual operation. Most research on this topic investigated the effect of mold heat transfer on quality and breakouts considering a particular casting variable, such as mold powder properties, casting speed, or steel composition [6-9]. Xia et al [7] investigated the dependence of integral heat flux on these casting variables, and used the results to analyze breakouts. Cicutti et al [8] developed an equation to predict mold heat flux (averaged over the hot face) as a function of these casting variables by performing multiple regression using data collected from a conventional slab caster producing low and medium carbon steels. Hetch et al [9] studied the effect of super heat, oscillation mark depth and mold powder consumption in addition to the effect of steel composition on mold heat removal, and investigated surface quality of crack sensitive steel grades as a function of mold heat flux. These papers all studied conventional slab casters. Santillana [10] et al studied the effect of casting powder and mold plate thickness on mold heat transfer in a thin slab caster, using plant measurements and the CON1D model[11] to simulate temperature in the strand and mold.

Data analysis techniques are extensively used to identify relationships between process variables and in developing models for predicting process outcomes [7-9]. In continuous casting of steel, there are significant opportunities for comprehensive study of plant measurements of the wide range of casting variables and their relationship to safety, quality, and production goals. This paper applies data fundamental analysis methods to predict mold heat flux in a thin slab caster as a function of casting conditions, based on extensive plant measurements of over 2 years at the Nucor steel mill in Decatur, AL. Different empirical equations to predict mold heat flux are developed with nonlinear multiple regression analysis. Based on statistical analysis, the models are evaluated and compared with a previous equation in the literature. The best models are presented, and can be applied to predict mold heat transfer in future work to understand and improve the continuous casting process.

METHODOLOGY

The Nucor Decatur steel mill has two Compact Strip Production (CSP) slab casters with a slab thickness of 90 mm, respectively called the North and South casters. The mill maintains a large data base of measurements of various conditions in the casters, most recorded every 5 seconds. The goal of the present work is to utilize this database to learn about and model the relationships between heat flux in the mold and these measurements. First, the effect of individual casting conditions on mold heat flux is studied by selectively filtering the data so that all other pertinent casting conditions are as constant as possible. Then, a model to predict mold heat flux as a function of casting variables is developed using nonlinear multiple regression. This is accomplished in four steps: data extraction, data pre-processing, model development, and evaluating the models.

Data extraction

Since the molds of continuous casters are constantly cooled by water, the spatially-averaged heat flux extracted from a mold hot face (hereafter simply called mold heat flux) at a given time can be calculated from measurements of the volumetric flow rate and temperature rise of the cooling water as

$$Q = \frac{G \cdot \rho_w \cdot C_w \cdot \Delta T}{10^6 \cdot 60 \cdot W \cdot Z} = \frac{6.794 \cdot 10^{-5} \cdot G \cdot \Delta T}{W \cdot Z} \tag{1}$$

where Q is the heat flux (MW/m^2), G is the flow rate (l/min), ρ_w is the density (kg/l), C_w is the specific heat capacity (J/kg °C), and ΔT is the temperature rise (°C) of the cooling water for a mold face with working (i.e. in contact with steel) length Z (m) and strand width W (m).

Measurement data is stored in the Level II database of the Nucor mill. Structured Query Language (SQL) is employed to extract the required data, which is located in different tables of the database. The query utilizes appropriate candidate keys (primary columns such as heat number) to cross-reference the data from different tables and to reduce the run time.

This work analyzed 16,000 heats on each caster over 2 years, covering a wide range of operating conditions. A heat at Nucor Decatur typically lasts around 50 minutes. To characterize the measurements of casting conditions during each heat, the measured data were averaged over a 10 minute interval, starting 20 minutes after ladle open so as to exclude transient effects during ladle changes. Heats that did not last this long, for example due to a breakout occurring, were not included. Data at every 5 seconds were extracted using SQL code and the average, maximum, and minimum of the 120 measurements over the 10 minute interval were computed and saved. In addition, the standard deviation was calculated for the mold level. The mold powder properties are reported by plant metallurgists, including the breakpoint temperature (which is considered a measure of the crystallization or melting temperature), and the viscosity. The final version of the query contains 150 lines of SQL code and takes less than 50 seconds to collect 2 years of data.

Data preprocessing

Pre-processing is a very crucial step in data modeling, in order to remove incomplete, noisy and inconsistent data that would distort the final model. To restrict the study to heats with steady casting conditions and reliable measurements, “primary filters” were applied, which required each selected heat to satisfy the conditions summarized in Table I. In the table, “variation” is the difference between the maximum and minimum measured value during the 10 minute interval selected for each heat.

Table I. North caster: Primary filters for casting variables

Casting variable	Filter criterion	Remaining heats (of 14135 total)
Constant casting speed	variation in $V_c \leq 2$ mm/s	13137
Mold powder type	excluding trial powders	13125
Constant mold width	variation in $W \leq 1$ mm	10723
Realistic super heat	$0 \leq s \leq 50$ °C	10558
Realistic mold level standard deviation	$l \leq 3$ mm	10556

Box plots and density plots for the collected data are shown in Figure 1, to visualize the distribution of values for each variable. To investigate the influence of each casting condition individually, by keeping the other conditions as constant as possible, a secondary filter is applied to every variable except for the one under investigation. A good secondary filter for a given variable (when not under individual investigation) should leave a large number of heats, with all measurements falling within a narrow range.

The secondary filters used in this work are given in Table II. The properties of the casting powders are tabulated in Table III.

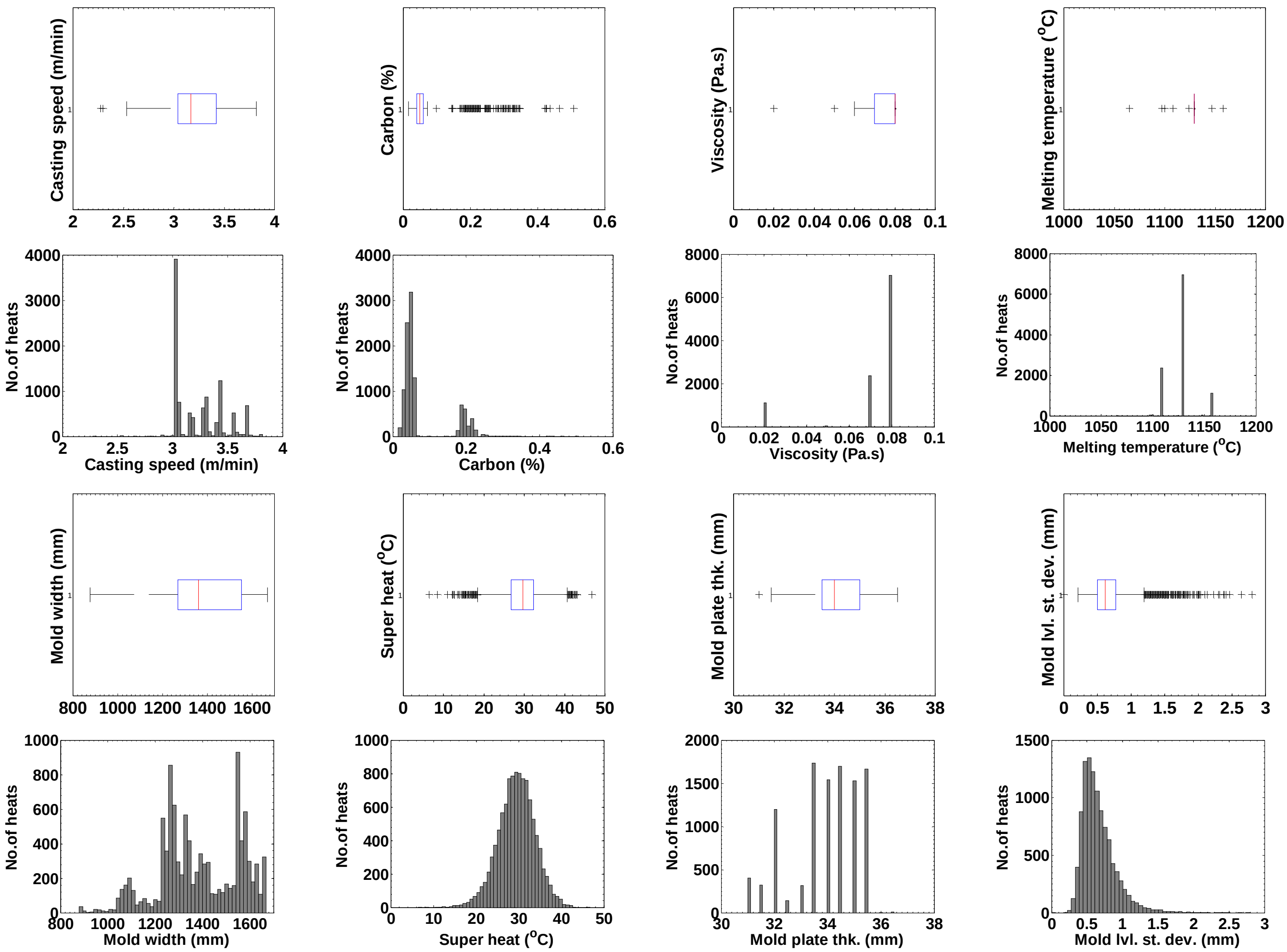

Figure 1. Box plots and density plots presenting data distribution of casting variables for fixed face of North caster at Nucor mill for two years

Table II. North caster: Operating conditions and secondary filters for casting variables

Casting variable	Measurement range (after primary filters)	Range for secondary filter
Casting speed (m/min)	2.27 - 3.71	3.02 - 3.05
Carbon percent (%)	0.015 - 0.507	0.0348 - 0.0545
Mold powder	see Table III	P4
Mold width (mm)	877.6 - 1668.8	1540 - 1590
Super heat (°C)	6.45 - 46.74	27 - 33
Mold plate thickness (mm)	31.0 - 36.5	33.5
Mold level standard deviation (mm)	0 - 2.8	0.447 - 0.615

Table III. Mold powder properties

		(calculated at 1300 °C)	
Powder	Basicity	Viscosity (Pa-s)	Break point temperature (°C)
P1	1.09	0.07	1108
P2	1.09	0.06	1124
P3	1.05	0.08	1147
P4	1.00	0.08	1129
P5	1.33	0.02	1158
P6	1.25	0.04	1127
P7	1.25	0.04	1128

Model development

The model development step starts by assuming a general structure for equations to predict mold heat flux as a function of casting variables. In general, numerical tools can determine parameters for the model that best fit the measurements, but not the structure of the model. For this work, the structure was partly based on an equation developed by Cicutti [8], stated in the literature:

$$Q = 4.63\cdot10^{6}\cdot\mu^{-0.09}\cdot T_{Flow}^{-1.19}\cdot V_c^{0.47}\cdot\left(1-0.152\cdot\exp\left(-\left(\frac{0.107-\%C}{0.027}\right)^{2}\right)\right) \tag{2}$$

where Q is the mold heat flux (kW/m^2), μ is the mold slag viscosity (Pa-s), T_{Flow} is the "melting temperature" of the powder (°C), V_c is the casting speed (m/min), and %C is the carbon amount (weight %). The expression inside parentheses accounts for the known drop in mold heat flux for peritectic steels. The predicted drop in heat flux is a bell-shaped (Gaussian) curve over Carbon content. The bell curve has a minimum at 0.107 weight % Carbon, where it subtracts a fraction of 0.152 (15.2 %) of the heat flux relative to a non-peritectic steel under the same conditions. The value 0.027 controls the width of the heat flux drop.

The current work extends the Cicutti equation to include other parameters according to the following structure:

$$Q = x_1\cdot V_c^{x_2}\cdot\mu^{x_3}\cdot T_{break}^{x_4}\cdot W^{x_5}\cdot s^{x_6}\cdot t^{x_7}\cdot l^{x_8}\left(1-0.152\cdot\exp\left(-x_9\left(\frac{\left(\frac{C_A+C_B}{2}\right)-\%C}{C_B-C_A}\right)^{2}\right)\right) \tag{3}$$

where Q is the predicted mold heat flux (MW/m^2). The fitting parameters x_i, i = 1, 2, .., 9 are chosen to best match the measurements. The variables, or measurements used as a basis for the prediction, are casting speed V_c (m/min), mold slag viscosity μ (Pa-s), break point temperature of the powder T_{break} (°C), width of the slab W (mm) , temperature superheat s (°C), thickness of the mold plate t (mm), standard deviation of the mold level l (mm), and carbon amount %C (weight %). Rather than using Cicutti's expression to incorporate the heat flux drop for peritectic steels, Eq. 3 gives this drop as a function of %C, including the effects of other alloys from the relation of Blazek et al [12]. Specifically, C_A and C_B determine the range of peritectic steels depending upon the measured composition of each heat as follows.

$$\begin{aligned}C_A = {} & 0.0896+0.0458Al-0.0205Mn-0.0077Si+0.0223Al^2-0.0239Ni+0.0106Mo+\\ & 0.0134V-0.0032Cr+0.00059Cr^2+0.0197W\end{aligned} \tag{4}$$

$$\begin{aligned}C_B = {} & 0.1967+0.0036Al-0.0316Mn-0.0103Si+0.1411Al^2+0.05Al\cdot Si-0.0401Ni+\\ & 0.03255Mo+0.0603V+0.0024Cr+0.00142Cr^2-0.00059Cr\cdot Ni+0.0266W\end{aligned} \tag{5}$$

where Al , Mn , Si , etc., are the element weight percentages of the steel composition in each heat.

Then, non-linear regression analysis is performed in MATLAB [13] to find the best fit values for the parameters that minimize the error (specifically the sum of squares of the differences between each measured heat flux and the predicted value from Eq. 3) using the 10556 heats after applying primary filters.

The minimization is performed using *fminsearch* function in MATLAB which employs the Nelder-Mead Simplex algorithm [14]. This function is sensitive to the initial guess. Therefore, to determine a good initial guess, a linear regression is first performed in Microsoft Excel, by taking the logarithm to make Eq. 3 linear. Then, nonlinear regression is performed in MATLAB for 100 initial guesses randomly distributed in the neighborhood of the linear best fit.

Initially, the significance of each of the eight casting variables included in Eq. 3 on mold heat flux is not clear. So, to find the best model, this analysis is performed with different combinations of casting variables. With eight variables, there are 256 different potential models, considering all possible combinations. Rather than test every combination, stepwise forward selection is used. Models are developed in a sequence, beginning with a model with only one casting variable. In each subsequent model, the one new casting variable that results in least RSS error is added into the equation [15].

Model evaluation

Among the different models from this stepwise forward selection, the best model is selected, accounting both for accuracy and simplicity, based on statistical measures, namely the residual sum of squares (RSS) and Akaike Information Criterion (AIC).

The residual sum of squares (RSS) is a measure of discrepancy between the data and estimation model. It is calculated as the sum of squares of the differences between the observed and predicted values.

$$RSS = \sum_{i=1}^{n} (y_i - f(x_i))^2 \tag{6}$$

where y_i is the observed value and $f(x_i)$ is the model predicted value, and n is the total number of observations. A smaller RSS indicates a better fit.

The coefficient of determination (R^2) is the ratio of explained variation to the total variation of the data and expresses the goodness of fit of a regression as follows.

$$R^2 = 1 - \frac{\sum_{i=1}^{n} (y_i - f(x_i))^2}{\sum_{i=1}^{n} (y_i - \bar{y})^2}, \quad \bar{y} = \frac{1}{n}\sum_{i=1}^{n} y_i \tag{7}$$

R^2 always lies between 0 and 1, with 1 indicating a perfect prediction of all data, and 0 indicating extreme variability. In this work, it is only employed to examine the relationship between mold heat flux and individual casting variables.

It is always possible to decrease RSS by increasing the number of variables in the model, even if the variable does not really contribute to the accuracy of the prediction. Other statistical measures, such as AIC, which penalizes adding insignificant variables, are better for comparing different model structures.

The Akaike Information Criterion (AIC) [16] is a measure of the relative quality of a statistical model. The AIC for a model is,

$$AIC = -2L + 2k \tag{8}$$

where L is the maximum likelihood of the measured data occurring given the "best" possible set of parameters, and k is the number of parameters. Using RSS as a measurement of the total error, the maximum likelihood corresponds to the smallest possible RSS, i.e. with the best fit parameters. Using this minimum RSS, the maximum log-likelihood value can be calculated as

$$L = -\frac{n}{2}\ln\left(\frac{RSS}{n}\right) \tag{9}$$

AIC measures the trade-off between the goodness of fit and complexity of the model. A smaller AIC indicates a better model.

The models are developed using fixed face of Nucor North caster, which is treated as training data. The models are then tested with data from the loose face of the North caster and both faces of the South caster. The performance of the optimum model to predict mold heat flux is then compared to the Cicutti prediction (Eq. 2) for the fixed faces of North and South casters.

MODEL VERIFICATION

Before developing a practical model with the complete database, the procedure for choosing best fit parameters described in the previous section is verified with a known equation, calculating the average heat flux for 1000 heats assuming a mold heat flux model form:

$$Q = x_1 \cdot G^{x_2} \cdot \Delta T^{x_3} \cdot W^{x_4} \tag{10}$$

where G is the water flow rate (l/min), ΔT is the rise in water temperature (°C) , and W is the mold width (m).

The influence of each of the above chosen variables on mold heat flux is shown in Figures 2-4. Regressions using only one (G), two (G and ΔT), and all three variables are shown in Figures 5-7 to illustrate the use of AIC in judging the model. With the addition of each variable, AIC drops indicating an improved model. There is only a moderate drop when the second variable is included, but a large drop when all three variables are included. This illustrates a problem in modelling nonlinear relationships, that it is difficult to separate the effects of the parameters. In addition, trends may appear weak and predictions poor if even one important and cross-correlated variable is missing from the model.

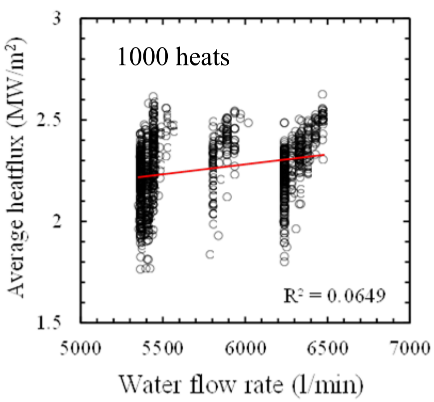

Figure 2. Increase in heat flux with water flow rate

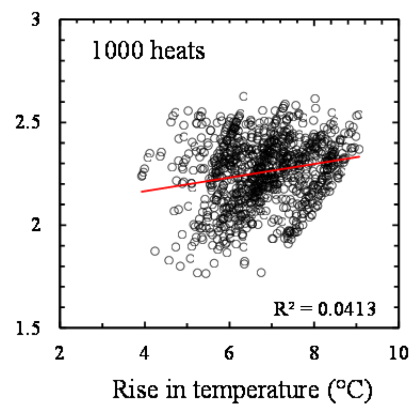

Figure 3. Variation in heat flux with rise in water temperature

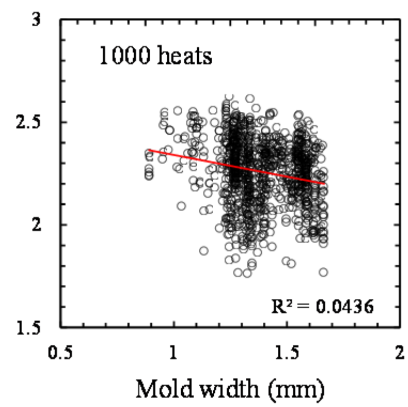

Figure 4. Variation in heat flux with mold width

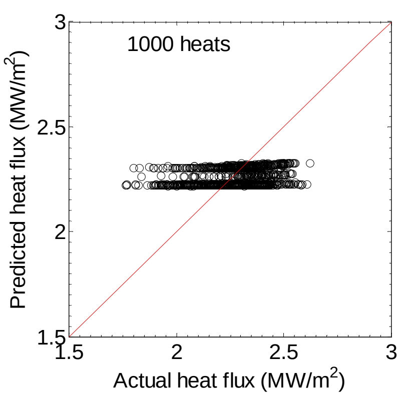

Figure 5. Regression with only water flow rate as a variable. AIC = -3730

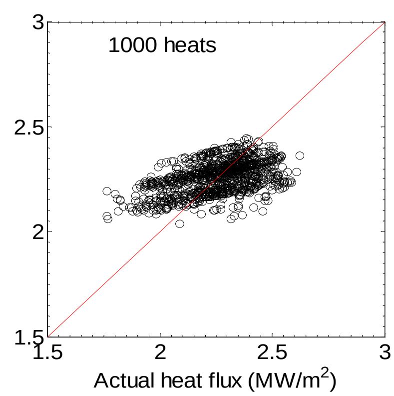

Figure 6. Regression with water flow rate and rise in temperature as variables. AIC = -3920

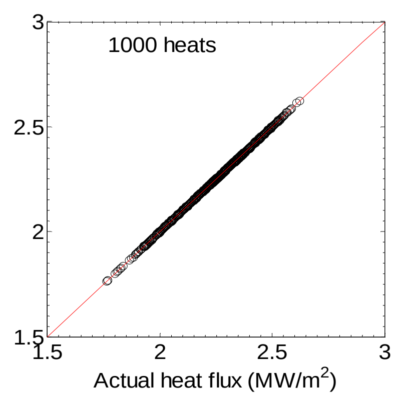

Figure 7. Regression with all 3 variables. AIC = -14337. Perfect match of predicted heat flux with actual heat flux

The best fit for x_i are $7.973 \cdot 10^{-5}$ ($\approx 6.794 \cdot 10^{-5} / 0.850$), 1, 1 and -1 respectively which exactly match those of the original equation (Eq. 1), given the fixed working mold length of 850 mm. Thus, the procedure is reliable.

RESULTS AND DISCUSSION

Heat extraction from the four mold faces is compared in Figures 8 and 9. Figure 8 shows larger heat flux from the wide faces than the narrow faces, in agreement with previous studies [8]. Figure 9 shows that there is no significant difference in the heat flux extracted between fixed and loose wide faces. Therefore, model development was performed using only the fixed face data. The loose face was used as testing data for comparing the developed models.

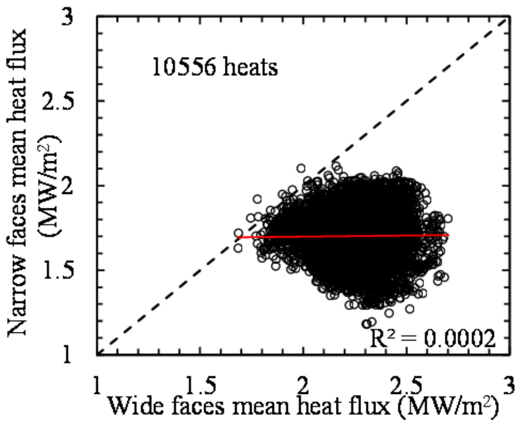

Figure 8.Total of average heat flux on two narrow faces versus total of average heat flux on two wide faces

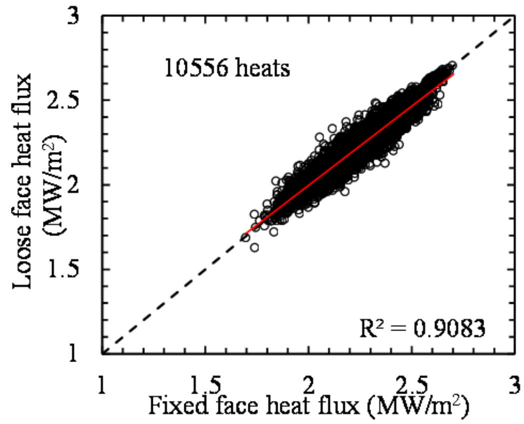

Figure 9. Comparison of heat flux between loose and fixed sides of wide face

Influence of individual variables

In order to investigate the influence of each of the eight casting variables on mold heat flux, the effect of other casting parameters must be made as insignificant as possible. In the current work, this was done by applying respective secondary filters to make all variables, except the one under study, as constant as possible, as described in the methodology section.

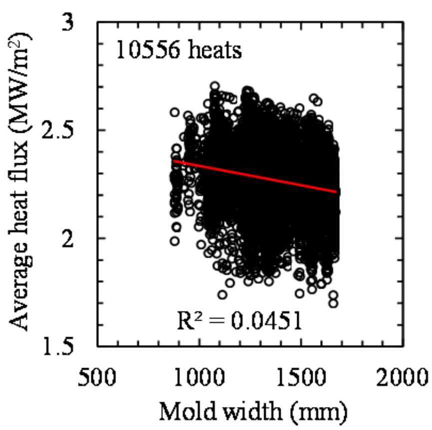

Figure 10. Average heat flux plotted against mold width after applying primary filters

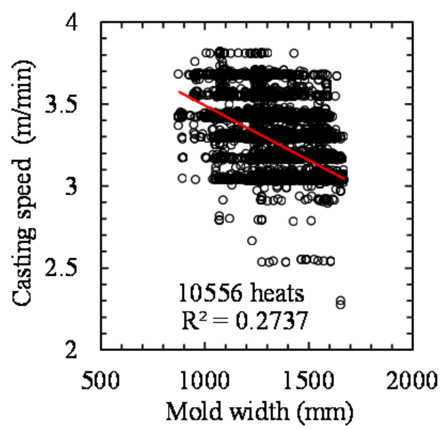

Figure 11. Variation of casting speed with mold width after applying primary filters

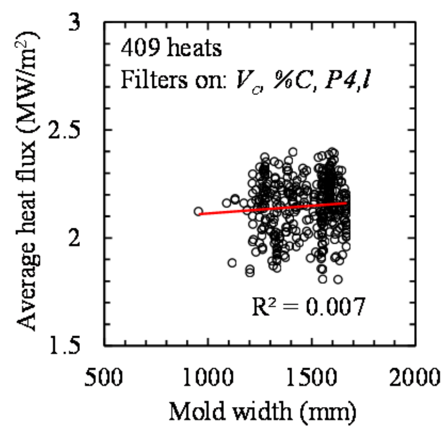

Figure 12. Variation of heat flux with mold with after applying secondary filters

An illustration of why this is important is provided in Figures 10-12. In Figure 10, the heat flux is plotted against mold width for every heat in the entire data set, with only primary filters applied to ensure reliable, steady measurements. The linear regression shows that heat flux tends to decrease with mold width. However, intuitively, with increasing mold width, low heat flux at the corners will become less important as high heat flux at the region of good contact over the rest of the wide face becomes larger. Thus mold heat flux is expected to increase with increase in mold width, which is opposite of what is seen in the data. Figure 11 offers an explanation for this, showing cross-correlation between casting speed and mold width. The common practice is to decrease casting speed as mold width increases to maintain constant throughput for quality reasons. Since heat flux has a stronger dependence on casting speed, this leads to a net decrease in heat flux with increasing mold width as seen in Figure 10. However, Figure 12 shows that, when secondary filters are applied to make casting speed constant, there is a small positive correlation observed between heat flux and mold width, as expected.

There are other cross-correlations in the data, related to mold powders. Specific mold powders are selected for particular grades, and some mold powders are related in composition, leading to related properties (viscosity and break point). Also, there are only a small number of powders in the data set after primary filtering, so sparseness of data may also lead to false correlations. These are accounted for by studying measurements for only a single powder, using the secondary filters.

Casting speed

Casting speed has the most significant influence on mold heat flux, as observed in Figure 13, which is well known from many previous studies [7,8,17]. As casting speed is increased, the residence time of the steel in the mold decreases. This makes the solidifying steel shell thinner, causing steeper temperature gradients, leading to higher heat flux. The resistance to heat flow across the gap between the shell and mold also decreases, owing to the drop in mold powder consumption (kg/m^2) [11] .

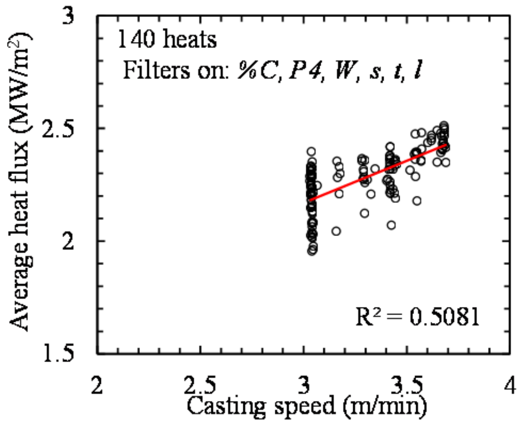

Figure 13. Increase in mold average heat flux with increase in casting speed

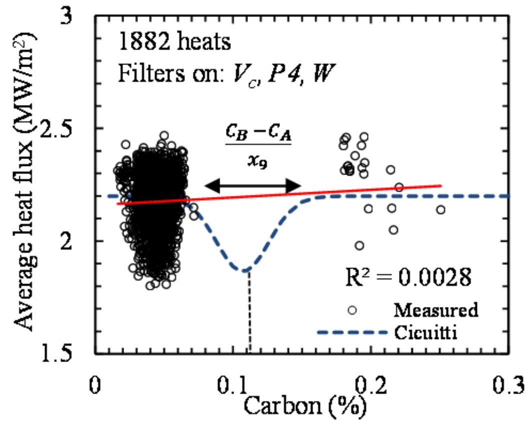

Figure 14. Effect of carbon on average heat flux

Carbon content

It is well known [7-9,18] that less heat is removed for peritectic steels compared to lower and higher carbon steels. The larger contraction of the steel during the peritectic phase change increases the gap between the shell and mold face resulting in lower heat flux. However, the Nucor Decatur mill does not cast peritectic steels. As shown in Figure 14, this effect cannot be observed from the data. For general application of the model to other casters, the term and variable (%C) accounting for this effect of steel composition was retained.

Mold powder properties

Mold powder properties are known to have a considerable influence on mold heat flux [7,8,19]. In this work, the different mold slag properties are characterized by the viscosity and break point temperature. Figure 15 shows that, as reported in the literature [19], higher break point temperature correlates with a lower heat flux. This heat flux drop occurs because a thicker solidified slag layer forms between the liquid slag layer and the mold, which increases the gap resistance.

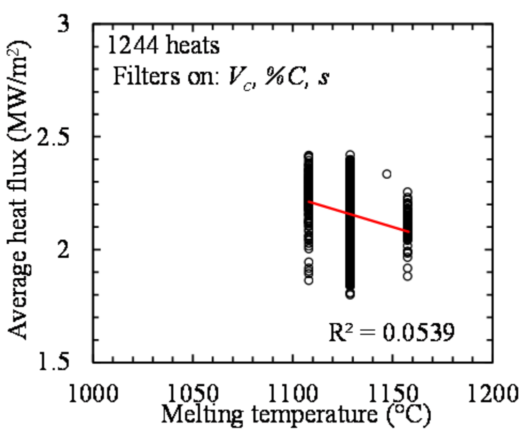

Figure 15. Mold heat flux decreases as break point temperature of mold powder increases

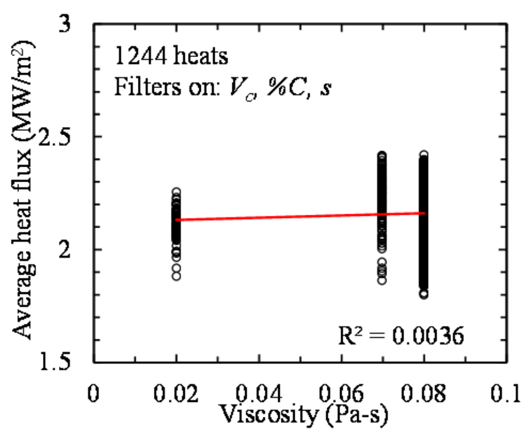

Figure 16. Variation of mold heat flux with viscosity of mold powder

Figure 16 shows a very slight effect of mold heat flux increasing with increasing slag viscosity. This disagrees with previously reported results [7,8,19] that higher viscosity is related to lower heat flux. This is likely due to cross-correlations and the small data set for mold powders, as described previously.

Mold width

Figure 17 shows a small increase in mold heat flux with increasing mold width. As discussed at the beginning of this section, this is likely due to the drop in heat flux at the mold corners becoming less important as the length of the region of good contact increases.

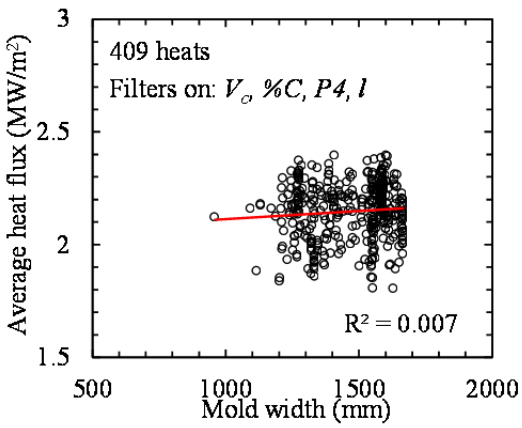

Figure 17. Influence of mold width on mold heat flux

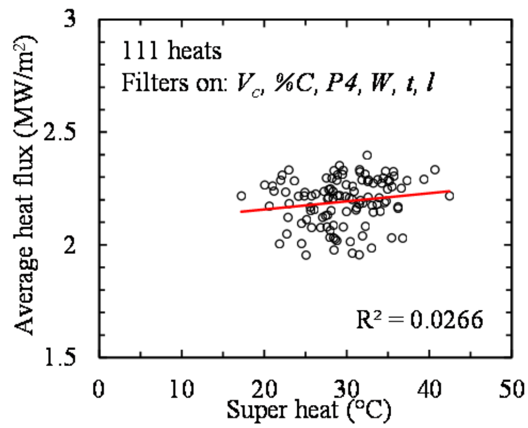

Figure 18. Effect of super heat on mold heat flux

Superheat

Figure 18 shows that mold heat flux increases very slightly with increasing superheat of the incoming liquid steel. This is expected because the higher corresponding liquid temperatures at the top surface should lessen meniscus freezing and hook formation, leading to shallower oscillation marks and less gap resistance. However, superheat temperature is measured in the tundish, leading to scatter, so the observed effect is very small, even after making other casting parameters as constant as possible to isolate the effect. This is in agreement with a previous study [9] which showed little effect of superheat on mold heat flux.

Mold level standard deviation

Figure 19 shows that increasing level fluctuations (as indicated by the standard deviation in mold level), leads to slightly lower heat flux. This is expected because higher mold level fluctuations result in deeper oscillation marks, increasing gap resistance, and thus reducing mold heat flux. As the standard deviation is less than 1 mm, the deviation measurements appear to be filtered for the benefit of the mold level control system, before being stored in the database. This may be why this trend is not observed in the data.

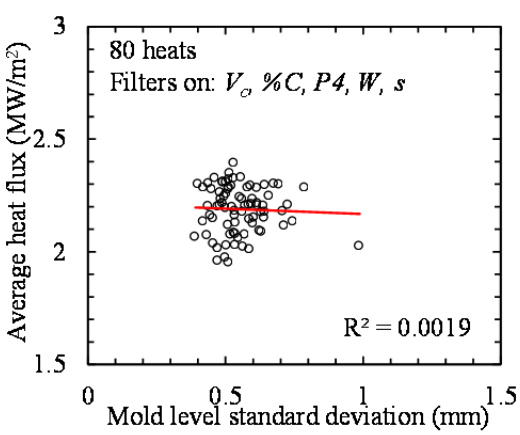

Figure 19. Variation of heat flux with mold level standard deviations

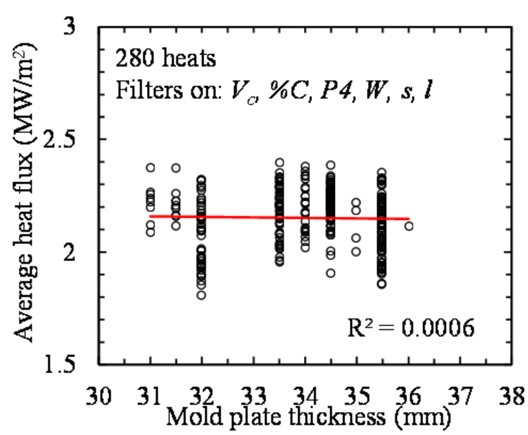

Figure 20. Little effect of mold plate thickness on mold heat flux

Mold plate thickness

It is expected that as mold plate thickness decreases, the resistance to heat flow decreases slightly, resulting in higher heat flux. Santillana et al [10] measured even higher than expected increase in mold heat flux as mold plate thickness decreases, owing to the increased hot face temperature of the mold decreasing slag layer thickness and further decreasing resistance to heat flow. But as shown in Figure 20, there appears to be little correlation between heat flux and measured mold plate thickness in this data. The effect is confounded by possible cross correlations because water flow rate may be adjusted with mold plate thickness.

In addition, plate thickness is measured only when the mold is changed, and therefore does not account for wear over the course of a campaign. As a proxy for this wear, Figures 21-24 show mold heat flux over the four longest campaigns in the data set plotted against the number of heats cast using that mold, using secondary filters for speed, composition and mold powder to account for changing casting conditions. There is a weak negative relationship, which may be due to the wear increasing surface roughness, and thus increasing gap resistance.

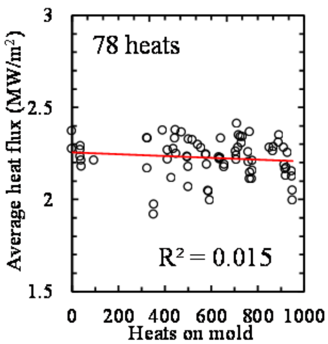

Figure 21. Slight decrease in heat flux with heats on mold for campaign 1

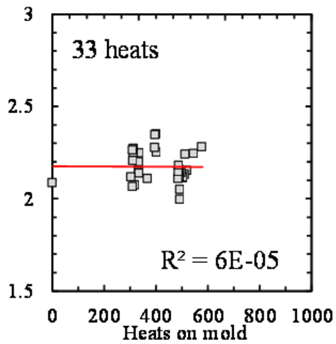

Figure 22. Effect not clearly seen for campaign 2

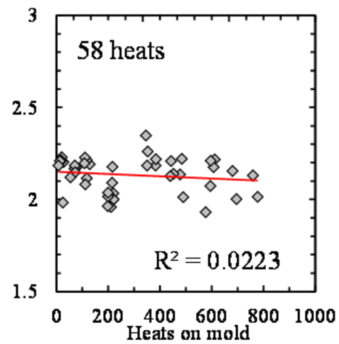

Figure 23. Slight decrease in heat flux with heats on mold for campaign 3

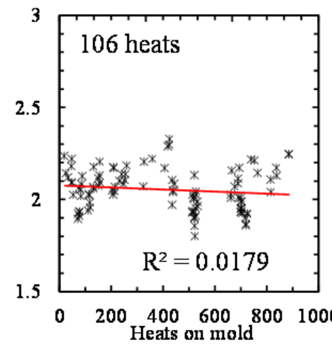

Figure 24. Slight decrease in heat flux with heats on mold for campaign 4

Model development and evaluation

The procedure described in the methodology section is performed to find best fit parameters for different combinations of casting variables. The results are summarized in Table IV. The successive models are developed through stepwise forward selection, meaning that the single variable that most decreases RSS is added to make the next model. The exception to this is the carbon term, as discussed below. RSS Error and AIC at each step illustrate the significance of the casting variable added.

As discussed in the individual effects section, some of these variables have strong cross-correlations with each other. These make it difficult for numerical techniques to converge to a unique set of best-fit parameters. There may be more than one set of best-fit parameters that give similar predictions. Therefore, including cross-correlated variables together, such as width and casting speed, may improve predictions of heat flux. However, it is difficult to extract conclusions about the underlying physics.

As seen above and in the literature, casting speed has a clear, strong influence on the average mold heat flux. Therefore, the first, simplest model is fitted with casting speed alone. Although the effect of carbon is not detectable with the current data set as peritectics are not cast at Nucor Decatur, for general application of the model to other casters, the carbon term is important. Therefore, the second model included casting speed and the expression accounting for drop in heat flux for peritectic grades. RSS did not decrease and AIC increased from model 1 to model 2, due to the lack of data, but the peritectic expression is included in the remaining models for generality to other casters.

The remaining variables were added in stepwise order. A decrease in RSS and AIC with the addition of break point temperature, width, viscosity and mold level deviation in the respective order indicate their inclusion is significant. But the contribution of viscosity and mold level deviation is very small. In fact, though heat flux appeared to have little correlation with viscosity, as shown in Figure 16, model 5 shows that there is a weak decrease in heat flux as viscosity increases. Based on AIC, model 8 appears to be the best predictive model.

Table IV. Different equations with statistical estimates

	Equation	RSS Error	AIC
1	$Q = 1.197 \cdot \mathbf{V_c^{0.544}}$	142.24	-45461.65
2	$Q = 1.411 \cdot V_c^{0.544} \cdot \left(\boldsymbol{1 - 0.152 \times exp\left(-0.0 \times \left(\frac{\frac{C_A + C_B}{2} - \%C}{(C_B - C_A)} \right)^2 \right)} \right)$	142.24	-45460.02
3	$Q = 33.708 \cdot 10^3 \cdot V_c^{0.543} \cdot \boldsymbol{T_{break}^{-1.434}} \cdot \left(1 - 0.152 \cdot \exp\left(-0.0 \cdot \left(\frac{\frac{C_A + C_B}{2} - \%C}{(C_B - C_A)} \right)^2 \right) \right)$	125.67	-46765.49
4	$Q = 22.747 \cdot 10^3 \cdot V_c^{0.613} \cdot T_{break}^{-1.462} \cdot \mathbf{W^{0.070}} \cdot \left(1 - 0.152 \cdot \exp\left(-0.0 \cdot \left(\frac{\frac{C_A + C_B}{2} - \%C}{(C_B - C_A)} \right)^2 \right) \right)$	122.54	-47030.08
5	$Q = 3.128 \cdot 10^5 \cdot V_c^{0.620} \cdot T_{break}^{-1.845} \cdot W^{0.072} \cdot \boldsymbol{\mu^{-0.017}} \cdot \left(1 - 0.152 \cdot \exp\left(-0.021 \cdot \left(\frac{\frac{C_A + C_B}{2} - \%C}{(C_B - C_A)} \right)^2 \right) \right)$	121.28	-47137.06
6	$Q = 1.788 \cdot 10^5 \cdot V_c^{0.618} \cdot T_{break}^{-1.759} \cdot W^{0.068} \cdot \mu^{-0.014} \cdot \mathbf{l^{0.008}} \cdot \left(1 - 0.152 \cdot \exp\left(-0.0 \cdot \left(\frac{\frac{C_A + C_B}{2} - \%C}{(C_B - C_A)} \right)^2 \right) \right)$	120.81	-47175.74
7	$Q = 2.848 \cdot 10^5 \cdot V_c^{0.615} \cdot T_{break}^{-1.827} \cdot W^{0.063} \cdot \mu^{-0.015} \cdot l^{0.08} \cdot \mathbf{s^{0.015}} \cdot \left(1 - 0.152 \cdot \exp\left(-0.002 \cdot \left(\frac{\frac{C_A + C_B}{2} - \%C}{(C_B - C_A)} \right)^2 \right) \right)$	120.57	-47194.59
8	$Q = 6.241 \cdot 10^5 \cdot V_c^{0.619} \cdot T_{break}^{-1.905} \cdot W^{0.065} \cdot \mu^{-0.016} \cdot l^{0.009} \cdot s^{0.011} \cdot \mathbf{t^{-0.072}} \cdot \left(1 - 0.152 \cdot \exp\left(-0.021 \cdot \left(\frac{\frac{C_A + C_B}{2} - \%C}{(C_B - C_A)} \right)^2 \right) \right)$	120.23	-47222.49

Another measure of performance of the new model equations, originally fit to data from the fixed face of the North caster, is to test their accuracy in predicting the loose face of the North caster and both faces of the South caster. Figure 25 compares the RSS errors for these models and Cicutti's equation (Eq. 2) on these four mold faces. The models developed in the current work give better predictions than the Cicutti equation. Due to symmetry between the faces, these models predict well for the North caster loose face.

There is an increase in RSS for both faces of South caster on addition of mold level deviation, superheat, and mold plate thickness. The respective variables may not have significant effect on heat flux, the effect may be different in magnitude between the two casters, the way they are included in the equation could need modification, or the measurements may be too inaccurate to discern the effect. For example, mold plate thickness is measured only at the start of a campaign, and whatever wear occurs during the campaign is not measured.

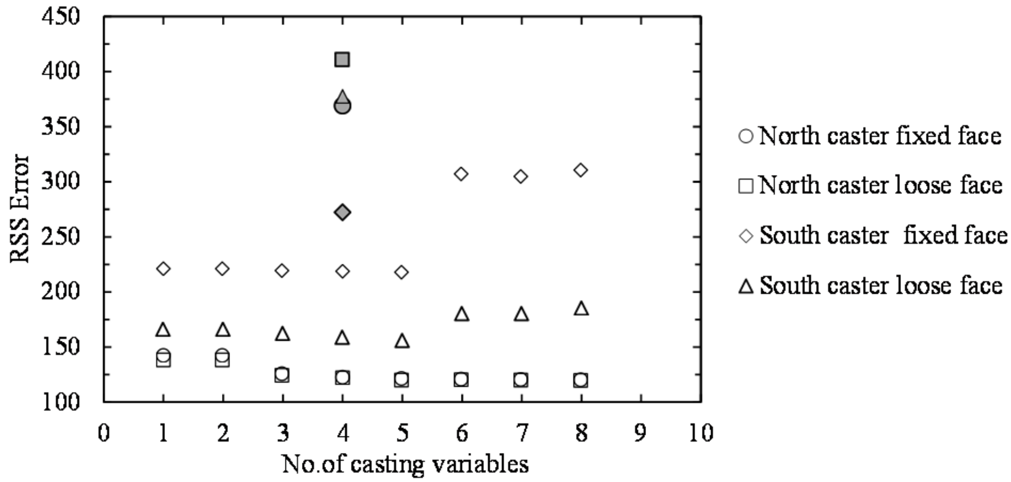

Figure 25. Performance of predicting equation on other casters; white markers are for models in Table IV, grey markers are for Cicutti equation (Eq. 2)

Thus, model 5, which is the best model before the jump in RSS, is considered to be superior to the other equations with respect to simplicity and accuracy shown again as follows.

$$Q = 3.128 \cdot 10^5 \cdot V_c^{0.620} \cdot T_{melt}^{-1.845} \cdot W^{0.072} \cdot \mu^{-0.017} \cdot \left(1 - 0.152 \cdot \exp\left(-0.021 \cdot \left(\frac{\frac{C_A + C_B}{2} - \%C}{(C_B - C_A)}\right)^2\right)\right) \quad (10)$$

This model is compared with the Cicutti equation graphically for the fixed faces of the North and South casters in Figure 26. The developed equation (Eq. 10) is clearly predicting better than the Cicutti equation.

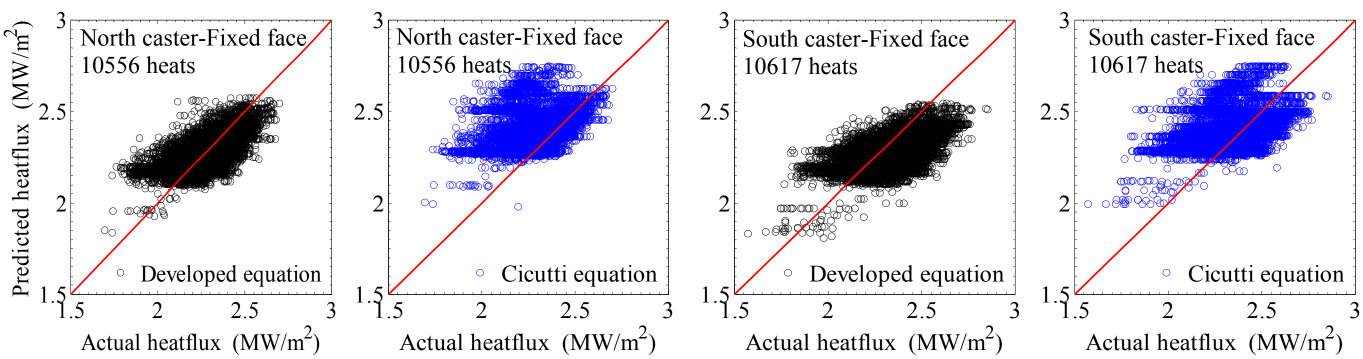

Figure 26.Comparison of new model 5 to Cicutti equation for fixed faces of North and South casters

The scatter still shows that this equation has room for improvement. One possibility is that the model needs to account for other casting variables, like mold oscillation mark depth and frequency, which are not considered in the present work. Better selection of casting variables, the structure of the model, and the handling of codependent variables could also lead to better results.

CONCLUSIONS

Average mold heat flux over the wide face of a thin slab casting mold is investigated using measurements of eight casting variables. Of the tested variables, casting speed has a clear, strong influence on heat flux. Break point temperature of mold powder, mold width and powder viscosity have a weaker effect that was not seen individually, but was found through nonlinear multiple regression of the data. The influence of carbon content is not observed because of non-availability of data for peritectic steels. The effect of superheat, mold plate thickness, and mold level standard deviation are not evident in the data, although no conclusion can be drawn about whether this is due to an actual lack of relationship, or a weakness in the data or methodology. An equation for predicting mold heat flux as a function of casting variables is developed. The developed model matches Nucor Decatur's casters better than the Cicutti equation, which was originally developed for a thick slab caster. Though characteristic to the plant, the equation is expected to behave well on other casters, due to its good performance on test data that was not used for model development. The results of this paper, being based on plant measurements, provide a greater understanding of mold thermal behavior, and the methodology can be extended easily to other casters and phenomena.

ACKNOWLEDGEMENTS

We would like to thank Ron O'Malley, Bob Williams, and others at Nucor Steel Decatur for providing access and valuable guidance for this project. We would also like to thank the members of the Continuous Casting Consortium at the University of Illinois at Urbana-Champaign for support of this research.

REFERENCES

1. R. B. Mahapatra, J. K. Brimacombe, I. V. Samarasekera, N. Walker, E. A. Paterson, and J. D. Young, "Mold behavior and its influence on quality in the continuous casting of steel slabs: Part i. Industrial trials, mold temperature measurements, and mathematical modeling", *Metallurgical Transactions,* Vol. B 22, No. 6, 1991, pp. 861-874.
2. T.J.H. Billany, A.S. Normanton, K.C. Mills, and P. Grieveson, "Surface cracking in continuously cast products", *Ironmaking and Steelmaking*, Vol.18, No.6,1991, pp. 403-411.
3. Hiraki, Sei, K. Nakajima, T. Murakami, and T. Kanazawa, "Influence of mold heat fluxes on longitudinal surface cracks during high speed continuous casting of steel slab", *In Steelmaking Conference*, Vol. 77, 1994, pp. 397-403.
4. Tada, Kichio, S. Kasai, Afcira Ichihara, and H. Onishi, "Improvement in Service Life of Continuous Casting Mold", *Kawasaki Steel Techinal Report,* No.17, 1987, pp. 26-33.
5. J.K. Park, B.G. Thomas, I.V. Samarasekera, and U. Sok Yoon, "Thermal and mechanical behavior of copper molds during thin-slab casting (I): Plant trial and mathematical modeling", *Metallurgical and Materials Transactions B: Process Metallurgy and Materials Processing Science*, Vol. 33, No. 3, June 2002, pp. 425-436.
6. W.H. Emling and S.Dawson, "Mold instrumentation for breakout detection and control", *Steelmaking Conference Proceedings*, Vol. 74, 1991, pp. 197-217.
7. G. Xia, H.P. Narzt and C. Furst , "Investigation of mould thermal behaviour by means of mould instrumentation", *Iron making and steelmaking*, Vol.31, No.5, 2004, pp.364-370.
8. C. Cicutti, M. Valdez, T. Perez, G. DiGresia, W. Balante, and J. Petroni, "Mould Thermal Evaluation in a Slab Continuous Casting Machine", *Steelmaking Conference Proceedings*, Vol. 85, 2002, pp. 97-107.
9. Hecht, Michael, Zhiyuan Zhu, Helmut Lachmund, and K. H. Tacke, "Mould investigations on a thick slab caster." *Revue de Métallurgie,* Vol. 102, No. 11, 2005, pp. 738-743.
10. B. Santillana, L.C. Hibbeler, B.G. Thomas, A. Hamoen, A. Kamperman, and W.V.D. Knoop, "Heat transfer in funnel-mould casting: effect of plate thickness", *ISIJ international*, Vol. 48, No. 10, 2008, pp.1380-1388.
11. Y.A. Meng, and B. G. Thomas, "Heat-transfer and solidification model of continuous slab casting: CON1D," *Metallurgical and Materials Transactions,* Vol. 34, No. 5, 2003, pp. 685-705.
12. K.E. Blazek, O. Lanzi III, P.L. Gano, and, D.L. Kellogg, "Calculation of the peritectic range for steel alloys", *Iron & steel technology,* Vol. 5, No. 7, 2008, pp. 80-85.
13. J.A. Nelder and R. Mead, "A simplex method for function minimization",*Computer Journal*,Vol. 7, No. 4, 1965, pp.308-313.
14. "Optimization Toolbox, User's Guide R2013 b, MATLAB", *The MathWorks*, 2010, pp.6-13.
15. J.A. Morgan, J.F. Tatar, "Calculation of the residual sum of squares for all possible regressions", *Technometrics*, Vol.14, No. 2, May 1972, pp. 317-325.
16. John I. Marden, "Multivariate Statistics Old School", Department of statistics, University of Illinois at Urbana-Champaign, 2012, pp.168-172.
17. M. Sadat, A. Honarvar Gheysari, and S. Sadat, "The effects of casting speed on steel continuous casting process", *Heat and Mass Transfer*, Vol. 47, No. 12, 2011, pp. 1601-1609.
18. S.N. Singh and K.E. Blazek, "Heat transfer and skin formation in a continuous-casting mold as a function of steel carbon content", *Journal Of Metallurgy*, Vol. 26, No.10, October 1974, pp.17-23,26.
19. K. Watanabe,M. Suzuki, K. Murakami, H. Kondo, A. Miyamoto, and T. Shiomi. "The effect of crystallization of mold powder on the heat transfer in continuous casting mold", *Journal of the Iron and Steel Institute of Japan,* Vol. 83, No. 2, 1997, pp. 115-120.